Crystallization and Solid-State Structure of Random Polylactide Copolymers: Poly(L-lactide-*co*-D-lactide)s

S. Baratian,[†] E. S. Hall,[‡] J. S. Lin,[§] R. Xu,[†] and J. Runt*,[†]

Department of Materials Science & Engineering, The Pennsylvania State University, University Park, Pennsylvania 16802; Cargill-Dow Polymers, Minneapolis, Minnesota 55440; and Solid State Division, Oak Ridge National Laboratory, Oak Ridge, Tennessee 37831

Received June 27, 2000; Revised Manuscript Received April 9, 2001

ABSTRACT: This paper presents a continuation of our earlier research on the crystallization and solid-state structure of polylactide copolymers. The focus here is on random copolymers containing predominately L-lactide and small amounts (1.5, 3, and 6%) of D-lactide. As expected, degrees of crystallinity and spherulite growth rates decrease substantially with increasing D-lactide content in the copolymers. The importance of defect arrangement (isolated vs paired stereochemical defects) was demonstrated by comparison to our earlier research on L-lactide/*meso*-lactide copolymers. At a given degree of supercooling, measured lamellar thicknesses decrease significantly with increasing *R* stereoisomer concentration: e.g., by more than a factor of 2 (compared to poly(L-lactide)) for the 6% D-lactide copolymer. The results of small-angle X-ray scattering experiments indicate that a significant amount of noncrystalline material resides between lamellar stacks. Equilibrium melting points were estimated for the copolymers using the Gibbs−Thomson approach, and the values conform with predictions of the model of Wendling and Suter in the exclusion limit. Taken together with the significant reduction in lamellar thickness and crystallinity, these results point to substantial rejection of D-lactide (and *meso*-lactide) defects from *S* stereoisomer crystals. However, experiments by others on similar copolymers suggest that a significant amount of *R* (or *R*−*R*) isomers can be included in *S* crystals under certain crystallization conditions. Some speculation about the origin of these differences is presented.

Introduction

In recent years there has been renewed interest in crystallization and the resulting solid-state structure of random copolymers,[1−5] particularly as a result of the introduction of polymerization catalysts that are capable of producing well-defined polyolefin random copolymers. Random copolymers produced from lactide dimers have also been the subject of widespread interest.[6−9] Polylactides are biocompatible and bioresorbable and have been used as scaffolds in tissue engineering and in other biomedical applications.[10−12] In addition, since lactides can be derived from renewable agricultural sources (and decompose cleanly under compost conditions), there has been considerable interest in the potential for their large volume application in films, fibers, and coatings. The lactide produced from agricultural sources consists primarily of the *S* stereoisomer, and the resulting polymers are consequently of relatively high *S* isomer content and crystallizable. It is in fact the crystallinity of this family of polymers that is responsible for a number of its interesting properties. Lactide polymers are rarely composed exclusively of *S* stereoisomers but, depending on the polymerization conditions and monomer feed, contain a significant concentration of *R* stereoisomer counits. The *R* units are generally placed randomly in the chains and have a profound influence on ultimate properties.

In the present study we continue our earlier investigation of the crystallization and solid-state structure of high L-lactide content polylactide copolymers.[13,14] We focus here on L-lactide/D-lactide random copolymers, with particular interest in the role of defect size on crystallizability and microstructure, and the location of the stereochemical defects within the structure.

Experimental Section

It is important at the outset to clarify the terminology that will be used in this paper. Polymers containing lactic acid repeat units are synthesized via the ring-opening polymerization of one or more cyclic lactides; a lactide is composed of two lactic acid units and so possesses two chiral carbon atoms. Two stereochemical isomers are possible: the *S* and *R* configurations. The possible dimeric lactides will be referred to using the prefixes L-, D-, and *meso*-. When polymerized, L-lactide results in the placement of two *S* isomers in the chain. Likewise, D-lactide results in two *R* isomers, while *meso*-lactide results in the introduction of one *R* and one *S* unit.

Synthesis. Both L- and D/L-lactide (Aldrich Chemical Co.) were melted and mixed under nitrogen. Tin(II) octanoate catalyst was then added (10 000:1 lactide to tin), and the mixture was held at 180 °C for 4 h. Nuclear magnetic resonance analysis has determined that this reaction produces essentially random copolymers.[15] D-Lactide was introduced in the nominal amounts of 0, 1.5, 3, and 6%, resulting in copolymers with *R* stereoisomer contents of 0.3, 1.7, 3.0, and 6.2%. *R* concentrations in the polymers deviate slightly from the dimer feed, presumably due to racemization of a small amount of *S* stereoisomer during the polymerization.[16] *R* stereoisomer content was determined using chiral liquid chromatography. The polymerizations were terminated (and the molecular weight controlled) by the addition of low molecular weight PLLA oligomers. The resulting polymers were dissolved in dichloromethane, filtered, and precipitated in methanol. The samples were then dried at 80 °C for 36 h and kept under vacuum in a desiccator when not in use.

Number (M_n)- and weight (M_w)-average molecular weights were measured by gel permeation chromatography using Waters Ultrastyragel columns and tetrahydrofuran as the mobile phase. The *R* content and polystyrene-equivalent molecular weights of the copolymers used in this study are contained in the top portion of Table 1. The copolymers are

[†] The Pennsylvania State University.
[‡] Cargill-Dow Polymers.
[§] Oak Ridge National Laboratory.

10.1021/ma001125r CCC: $20.00
Published on Web 06/09/2001

Table 1. Nominal Comonomer Content, *R* Stereoisomer Content, and Molecular Weights for the Poly(lactide) Copolymers

	nominal comonomer content	% *R* isomer	M_n	M_w	no. av *S* run length
polymer A (PLLA)		0.4	65 500	127 400	
copolymer E	1.5% D-lactide	1.7	72 900	110 800	125
copolymer F	3% D-lactide	3.0	81 900	143 500	67
copolymer G	6% D-lactide	6.2	75 100	128 500	33
copolymer B	3% *meso*-lactide	2.1	65 800	122 600	54
copolymer C	6% *meso*-lactide	3.4	63 900	119 100	31
copolymer D	12% *meso*-lactide	6.6	65 500	121 300	16

labeled as A, E, F, and G in order of increasing *R* content. Polymer A is essentially poly(L-lactide), PLLA. As seen in the table, the molecular weights of the four polymers are very similar, so that differences in crystallization kinetics can be attributed directly to differences in optical composition. The calculated number-average run lengths of *S* stereochemical sequences[17] are also provided in Table 1.

Throughout the paper, comparison will be made to the results of a previous study on L-lactide/*meso*-lactide copolymers. These copolymers have been termed copolymers B, C, and D, and their characteristics are listed in the bottom half of Table 1. Their molecular weights are quite similar to each other and to the D-lactide copolymers. The average *S* stereoisomer run lengths of the *meso*-lactide copolymers are about half of that of the D-lactide copolymers since the defects are paired in the latter copolymers.

Sample Preparation. For optical microscopy experiments, samples were prepared by placing ~3 mg of copolymer powder on a microscope slide and inserting it into a Mettler model FP-82 hot stage, set to 30 °C above the sample's nominal melting point (T_m). As the polymer melted, a coverslip was placed on the molten polymer and pressed down onto the sample. The samples were then removed from the hot stage and allowed to cool to room temperature. For small-angle X-ray scttering (SAXS) experiments, a stainless steel mold was used to form the powdery polymer into a solid bar of dimensions approximately 6 cm × 1.5 cm × 0.2 cm. First, the mold was heated on a hot plate to a temperature 30 °C above the nominal T_m and the polymer powder placed in the mold and melted. The hot assembly was then placed into a Carver Laboratory hot press, maintained at 20 °C below the melting point so the polymer could slowly solidify during packing. A pressure of 10 000−11 000 psi was applied for 5 min to the mold and then reduced to ~2000 psi for 10 s. A final pressure of 20 000 psi was applied for 3 min, after which the mold was removed from the press and allowed to cool. The solid plaques was forced out of the mold and cut into ~1 cm × 1 cm samples.

Both types of specimens were isothermally crystallized in the same fashion, using two hot stages. The "melting" stage was set to 40 °C above the nominal T_m and the "crystallizing" stage set to the crystallization temperature (T_c). Each sample was placed in the melting hot stage for 3−5 min and then rapidly transferred to the crystallizing hot stage. Samples for SAXS analysis were crystallized over the following T_c ranges: material A, 120−147 °C; copolymer E, 115−154 °C; copolymer F, 118−142 °C; and copolymer G, 112.5−130 °C, for time periods in excess of the time required for complete crystallization (40 min−24 h).

For relatively high T_c's (i.e., within about 25 °C of the nominal T_m), primary nucleation was very slow, and a "self-seeding" approach was used to obtain spherulite growth rates.[13] The polymers were quenched from the melt to a temperature below the desired T_c for ~20 min in the crystallization hot stage. The hot stage was then set to the desired isothermal T_c, and 30 min after the sample stage reached that temperature, spherulite growth was recorded.

Optical Microscopy. An Olympus model BH-2 microscope and camera were used for recording morphologies and making spherulitic growth rate measurements. A video camera in combination with a VCR was used to record spherulite sizes as a function of time during isothermal crystallization. For each T_c, from 3 to 12 spherulites were monitored on 2−3 repeat samples. Spherulite radius vs time behavior was linear in all cases. The average spherulitic growth rates (G) were determined from the slope of the regression lines.

Calorimetric Measurements. Heats of fusion and melting temperatures for each SAXS sample were obtained at 10 °C/min using a Perkin-Elmer series 7 DSC. An average sample size of ~4 mg was used for the heat of fusion measurements. Baselines defining the melting endotherm of the highest melting specimen of a given copolymer were constructed by linearly connecting the point 20 °C below the first evidence of melting to that 10 °C beyond the conclusion of melting. Similar temperature limits were used for all other specimens of a given copolymer. Samples for determination of melting temperatures were obtained by slicing thin strips from the SAXS samples. Sample sizes were kept to a minimum: 0.2 ± 0.05 mg. These considerations allowed for good thermal contact with the sample pan and minimized thermal lag. As in our previous study of L-lactide/*meso*-lactide copolymers, single melting endotherms were generally observed for all specimens, and the melting peak temperature was independent of heating rate in the range 2.5−40 °C/min. Bulk crystallinities were determined by comparing the measured heat of fusion to the perfect crystal heat of fusion ($\Delta H_f°$) of PLLA (100 J/g). The value of 100 J/g was determined from experiments on highly crystalline PLLA.[13] The measured glass transition temperatures for poly(L-lactide) and all copolymers were near 56 °C.

Small-Angle X-ray Scattering. SAXS experiments were performed at the Oak Ridge National Laboratory on a 10 m pinhole-collimated SAXS camera. A Cu Kα radiation source (wavelength (λ) = 0.154 nm) and a 20 cm × 20 cm two-dimensional position-sensitive proportional detector were used to generate and collect data. The two-dimensional data were azimuthally averaged, converting the data to a one-dimensional profile. The sample scattering intensity was corrected for detector uniformity and efficiency, empty beam background scattering, and dark current. Absolute intensities were determined by comparing experimental scattered intensities to those of two well-defined secondary standards: a high-density polyethylene and a vitreous carbon.

Sample-to-detector distances of 1.119 and 5.119 m were used to collect data at high and low scattering angles, respectively. The data sets were suitably appended. The scattering from PLLA and the various copolymers was relatively low (due to the modest difference in the electron densities of the amorphous and crystalline regions), and the signal-to-noise ratio was relatively high in certain q ranges [$q = (4\pi/\lambda)\sin(\theta/2)$ and θ is the scattering angle]. Consequently, the data were smoothed using a moving window average procedure.[18] Since the experimental q range covered in the measurements includes the leading edge of the wide-angle diffraction, the background scattering was estimated (and removed from the experimental scattering) using the method of Vonk:[19]

$$I_b(q) = a + b(q)^4 \tag{1}$$

where a and b are fit parameters.

The one-dimensional correlation function, $\gamma(r)$, is used in the analysis of stacked lamellar structures to provide information about the long period (L), lamellar thickness (l_c), amorphous layer thickness (l_a), and the invariant. $\gamma(r)$ can be written as[20,21]

$$\gamma(r) = \frac{1}{2\pi^2}\int_0^\infty q^2 I(q)\cos(qr)\,\mathrm{d}q \tag{2}$$

where $I(q)$ is the experimental SAXS intensity and r is the correlation distance. After background subtraction, the scattered intensity decayed to zero beyond $q \sim 1.2$ nm^{-1} for all samples. The beam stop was observed to influence the scattering below $q = 0.1$ nm^{-1}, and all experimental data points below 0.1 nm^{-1} were discarded. For the purpose of calculating

$\gamma(r)$, "data" at low q were then created by linearly extrapolating from the data point at 0.1 nm^{-1} to zero q. No significant differences in the calculated correlation functions were observed when using this method vs either truncating the data directly to zero just below $q = 0.1$ nm^{-1} or mirroring the higher q data through the scattering maximum.

The general characteristics of the calculated $\gamma(r)$ are similar to those reported earlier for the L-lactide/*meso*-lactide copolymers as well as other semicrystalline polymers. The location of the first maximum in $\gamma(r)$ provides a measure of the long period. When the linear crystallinity (x_c) > 0.5, the intersection of the linear fit to the self-correlation portion of $\gamma(r)$ with $\gamma(r) = 0$ is r_0:

$$r_0 = l_c(1 - x_c) \tag{3}$$

and therefore

$$r_0/L = x_c(1 - x_c) \tag{4}$$

where x_c is defined as the ratio of the average lamellar thickness to the average long period. For $x_c < 0.5$, x_c is replaced by $(1 - x_c)$ in the above expressions. Although one cannot a priori distinguish x_c from x_a (= $1 - x_c$, the fraction of the amorphous layer in the stacks), secondary evidence can be used to provide a reasonable choice. This issue will be discussed at more length in the next section.

In the previous study of *meso*-lactide copolymers,[13] long periods used in the analysis of the linear crystallinity were determined from the Lorentz-corrected plots. To facilitate a direct comparison to the results reported in that paper, the same method was used here. The x_c values calculated from Lorentz-corrected intensities were not significantly different from those derived from the correlation functions. Once the linear crystallinity was determined, l_c and l_a were readily obtained from $l_c = Lx_c$ and $l_a = L(1 - x_c)$.

Results and Discussion

Bulk Crystallinity. Degrees of crystallinity for PLLA and copolymers E−G are presented vs T_c in Figure 1a and vs the corresponding degrees of supercooling, $\Delta T = T_m^0 - T_c$, in Figure 1b. T_m^0 is the equilibrium melting point of the particular (co)polymer in question—see a following section for discussion of how these were estimated. The data for the three *meso*-lactide copolymers from ref 13 (determined using the same baseline construction procedure and calibration standard) are also added to Figure 1a,b for comparison purposes. The solid lines in the figures are to help guide the eye and are not intended to imply a functional form for the data.

From Figure 1a,b it is evident that there is a significant decrease in the ability of the D-lactide copolymers to crystallize with increasing D-lactide content: φ_c ranges from ~45−65% for material A (PLLA) to 15−25% for copolymer G (6.2% *R* content). For PLLA and copolymers E and F the crystallinities increase with decreasing ΔT; hence, a greater degree of ordering is observed at higher T_c where crystal growth is slower. This behavior is similar to that of *meso*-lactide copolymers B and C as well as that of isotactic polypropylene copolymers containing stereo defects.[22]

Each D-lactide copolymer used in this study has an optical composition very near that of a corresponding *meso*-lactide copolymer in ref 13: compare copolymers E and B, F and C, and copolymers G and D (Table 1). Although the *R* stereoisomer content is the same within each pair, the *R* counits are paired in the case of the D-lactide copolymers but unpaired in the *meso*-lactide copolymers. Consequently, at equivalent *R* content, the

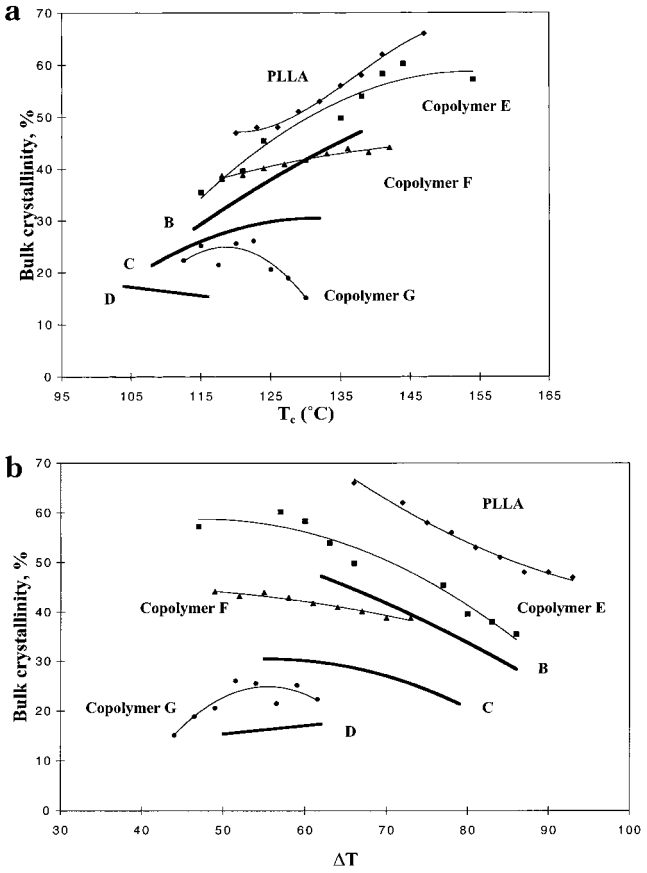

Figure 1. (a) Bulk degrees of crystallinity vs T_c. Material A, PLLA (◆), copolymers E (■),F (▲), and G (●). Data for the three *meso*-lactide copolymers from ref 13 are included for comparison purposes. (b) Bulk degrees of crystallinity vs degree of supercooling. PLLA (◆), copolymers E (■), F (▲), and G (●). Data for the three *meso*-lactide copolymers from ref 13.

meso-lactide copolymers contain effectively twice the number of randomly placed chain defects compared to the corresponding D-lactide copolymers, albeit that the defects in the D-lactide copolymers are twice as large.

The D-lactide copolymers have considerably larger average *S* sequence lengths at a given *R* counit content compared to the *meso*-lactide copolymers (see Table 1) and therefore higher degrees of crystallinity. This expectation is confirmed experimentally: compare the crystallinities of D-lactide copolymer E to *meso*-lactide copolymer B, copolymer F to C, and copolymer G to D. Clearly, arrangement of the *R* counits within the polymer chain plays a critical role in determining crystallizability. Finally, although the absolute optical compositions are quite different, D-lactide copolymer G and *meso*-lactide copolymer C possess a very similar concentration of chain defects (comonomer content). As seen in Figure 1a,b copolymer G generally exhibits somewhat lower crystallinity than copolymer C, presumably as a consequence of larger average defect size in G.

Lamellar Microstructure. Figure 2 displays the Lorentz-corrected SAXS intensity vs q for selected samples of copolymer E. The behavior of the other copolymers is very similar. The long periods ($L = 2\pi/q_{max}$) increase progressively with T_c for all materials. Weak second-order reflections are observed for several of the PLLA and copolymer samples, particularly at higher T_c, indicating relatively well-ordered lamellar stacks.

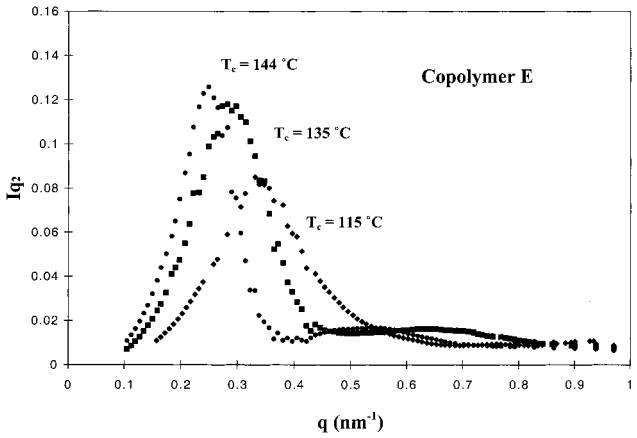

Figure 2. Scattered intensity vs q for copolymer E crystallized at 115 (◆), 135 (■), and 144 °C (●).

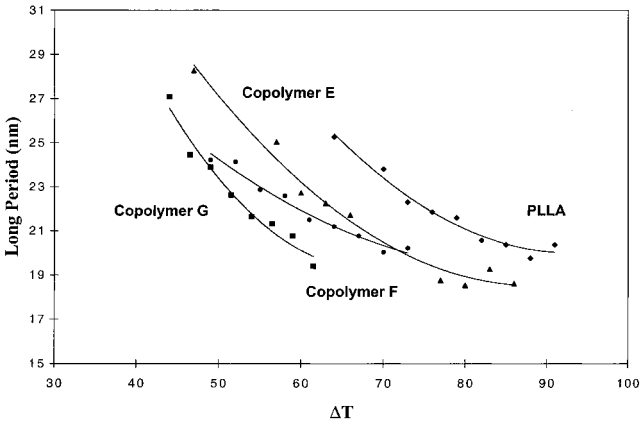

Figure 3. Long period vs degree of supercooling for PLLA (◆) and copolymers E (▲), F (●), and G (■).

Figure 3 presents the long periods for PLLA and the D-lactide copolymers vs ΔT. It is evident that increased defect concentration results in a significant decrease in L for materials crystallized at similar ΔT. This behavior is consistent with the reduction in lamellar thickness with increasing defect concentration, as will be discussed shortly.

The bulk crystallinities for PLLA and the D-lactide copolymers are in the range 15−60%, too low to assume that the amorphous component only resides in lamellar stacks like in the case of more highly crystalline homopolymers like poly(ethylene oxide).[23] Optical microscopy experiments show that volume-filling spherulites are obtained for all materials and T_c's investigated in this study; hence, there is no appreciable amount of material in interspherulitic regions.

As discussed earlier, l_c and l_a can in principle be derived from the correlation function, but secondary evidence must be used to distinguish between them (or between x_c and x_a). First, following from the definition of the linear crystallinity, $x_c \geq \phi_c$, where ϕ_c is the volume fraction crystallinity. [The case where $x_c = \phi_c$ indicates that essentially all of the amorphous material resides between lamellae and $l_c = L\phi_c$. $x_c > \phi_c$ indicates that a portion of the amorphous component resides in regions between lamellar stacks.] In addition, l_c is well-known to increase with increasing T_c. Preliminary estimates of lamellar thicknesses in these copolymers using tapping mode atomic force microscopy are consistent with the values derived from SAXS using the logic provided above.[24]

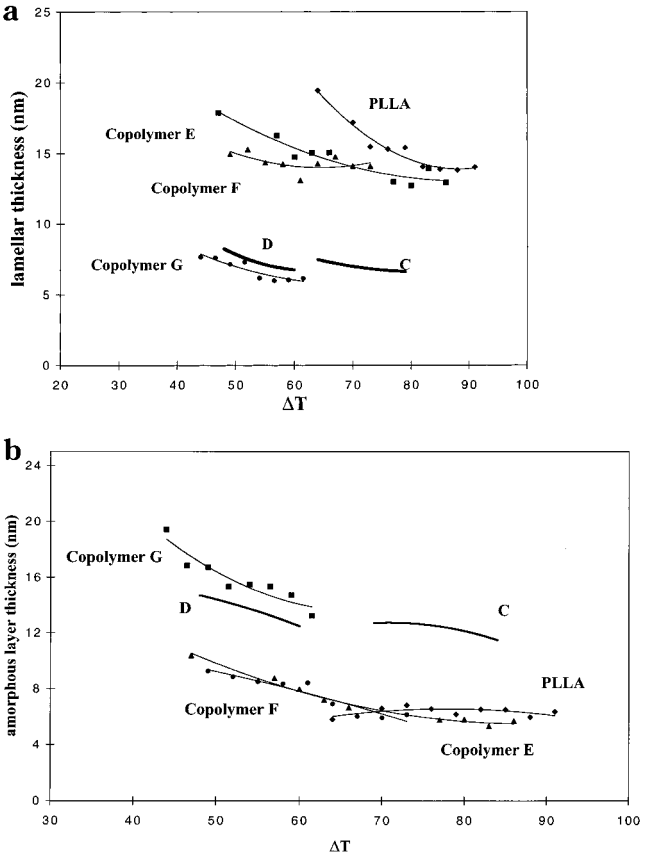

Figure 4. (a) Lamellar thickness as a function of ΔT. PLLA (◆), copolymers E (■), F (▲), and G (●). Data for the three *meso*-lactide copolymers from ref 13. **(**b**)** Amorphous layer thickness as a function of ΔT. PLLA (◆), copolymers E (▲), F (●), and G (■). Data for the three *meso*-lactide copolymers from ref 13.

Crystalline and amorphous layer thicknesses are plotted in Figure 4a,b vs ΔT. When using the correlation function to determine l_c (and l_a), there is considerable uncertainty in estimating x_c (and hence l_c) when x_c is near 50%. Consequently, only x_c values less than 0.4 or greater than 0.6 were used to calculate l_c and l_a. This was the same criteria as used in our previous study of the *meso*-lactide copolymers.[13] There were only two samples for which x_c fell between 0.4 and 0.6 in the present study, and l_c was consequently not estimated in these cases.

Figure 4a shows that there is a distinct reduction (by more than a factor of 2 for copolymer G) in lamellar thickness with increasing comonomer content. Similar behavior was observed previously for the *meso*-lactide copolymers, and that data is reproduced in Figure 4a. [There are no data points in the figure corresponding to copolymer B since $0.4 \leq x_c \leq 0.6$ for all samples.] Clearly, the degree of supercooling is not *the* primary factor controlling l_c, as it is for homopolymers, but comonomer content is critically important. Similar behavior has been reported for poly(propylene)s with different isotacticities.[22] Our results point to significant rejection of *R* counits from the crystalline lamellae.

In Figure 4b, the average amorphous layer thickness is seen to increase at higher comonomer concentrations, indicating that there is relatively more amorphous material incorporated into lamellar stacks at higher D-lactide levels. It is difficult to discern however whether there are any differences at lower defect concentrations.

For PLLA and all of the D-lactide copolymers, the linear crystallinity is greater than the bulk crystallinity, as is the case for the *meso*-lactide copolymers. This leads to a model for the solid-state structure in which the amorphous material resides in significant amounts in both interlamellar and interfibrillar regions. The fraction of the amorphous component residing in interfibrillar and interlamellar regions can be estimated as follows.[23] The volume fraction of lamellar stacks (v_s) is defined as $v_s = \varphi_c/x_c$, and the volume fraction of amorphous material not incorporated in the stacks is simply $1 - v_s$. The fraction of the amorphous component residing in interfibrillar regions (η_{if}) is then $= (1 - v_s)/(1 - \varphi_c)$, and the fraction in interlamellar regions is $1 - \eta_{if}$. For PLLA, the fraction of the amorphous component residing between fibrils increases from ~60% at low T_c to ~40% at higher T_c. A similar trend is observed for the copolymers, with η_{if} varying from about 20−70%, depending on T_c.

Equilibrium Melting Points. The equilibrium melting points of the copolymers are important parameters in the study of the crystallization of poly(lactide) copolymers and can in principle help to provide insight (albeit indirect) into the location of the D-lactide units in the microstructure. A variety of methods have been proposed and utilized to determine T_m^0 for various homo- and copolymers, and the utility of these approaches in the present case is reviewed briefly below.

The Gibbs−Thomson relationship for the melting of thin crystals is the most reliable means for estimating T_m^0 of lamellar crystals of sufficiently large lateral dimensions. This approach utilizes the correlation between lamellar thickness and crystal stability and can be written as[25]

$$T_m = T_m^0\left[1 - \frac{2\sigma_e}{\Delta H_f^0(l_c)}\right] \tag{5}$$

where T_m is the observed melting point for lamella of thickness l_c and σ_e is the end (fold) surface free energy. T_m^0 is estimated by extrapolation of T_m vs $1/l_c$ data to $1/l_c = 0$.

The most popular method for determining T_m^0 for homo- and copolymers is the Hoffman−Weeks approach, derived from eq 5 and several simplifying assumptions.[25] However, Hoffman−Weeks plots (T_m vs T_c) are sometimes curved, making unambiguous determination of an apparent T_m^0 difficult at best. In addition, it has been argued in recent papers that the conventional Hoffman−Weeks linear extrapolation for obtaining T_m^0 is not, in general, appropriate.[26,27] In addition, T_m (and l_c) is not "just" primarily dependent on ΔT but is also a strong function of comonomer content (see Figures 4a and 5b), a factor that is not taken into consideration in the usual Lauritzen−Hoffman−Miller (LHM) model of polymer crystal growth.[28]

T_m^0 determined via Gibbs−Thomson extrapolations for PLLA and the D-lactide copolymers are compiled in Table 2. The calculated statistical error associated with the extrapolated values is generally on the order of ±8 °C. Consequently, one has to be careful not to overinterpret the differences between the copolymers. Nevertheless, it is clear that the equilibrium (and experimental) melting points decrease significantly with increasing comonomer content. The scatter in the T_m vs $1/l_c$ data was significant for copolymer E, and a Gibbs−Thomson value is not reported in Table 2 due to the relatively large uncertainty.

Table 2. Equilibrium Melting Point Predictions from Copolymer Melting Models

material	exptl $T_m^{0\prime}$ (°C)	exclusion[32] (°C)	uniform inclusion[25] (°C)	modified exclusion[33] (°C)
copolymer F	191	203[a]/207[b]	206/208	187/198
copolymer G	174	194/202	200/206	166/186
copolymer B	200	205	207	194
copolymer C	187	202	205	185
copolymer D	166	193	200	164

[a] Based on *R* content. [b] Estimate using paired *R* defects.

The T_m^0 determined for PLLA is very similar to that reported previously.[13,29] σ_e was estimated from the slope of the Gibbs−Thomson plot to be ~63 erg/cm^2 for PLLA, compared with the value (53 erg/cm^2) reported by Hoffman et al.[30] based on a reanalysis of the spherulite growth rate data of Vasanthakumar and Pennings.[30] Like the *meso*-lactide copolymers, the apparent σ_e decreases to a value less than half of that PLLA at the highest comonomer content (~24 erg/cm^2). The origin of this reduction is unclear at present but strongly suggests that the nature of the crystal surface is changing with increasing comonomer content (perhaps associated with increasing defect concentration at the interface).

Experimental melting points for PLLA and the D-lactide copolymers are shown in Figure 5a vs T_c and in Figure 5b vs ΔT. T_m's for *meso*-lactide copolymers B−D are included in Figure 5b for comparison purposes. As expected, comparing the *meso*- and D-lactide copolymers at similar optical composition (i.e., copolymers E vs B, F vs C, and G vs D) confirms that the isolated defects in the *meso*-lactide copolymers lead to a greater reduction in T_m compared to the D-lactide copolymers. Comparing on the basis of comonomer content or similar number of defects (i.e., copolymer F vs B and copolymer G vs C), the larger D-lactide defects are seen to have a more significant impact on reducing T_m.

Melting Models: Random Copolymers. Several models have been proposed to account for changes in the equilibrium melting points of random copolymers as a function of the mole fraction of crystallizable units (X_S). Flory has shown that for complete exclusion of a second comonomer (*R*) from *S* crystals:[31]

$$\frac{1}{T_m^{0\prime}} - \frac{1}{T_m^0} = \frac{-R}{\Delta H_f^0}\ln X_S \tag{6}$$

where $T_m^{0\prime}$ is the equilibrium melting point of the copolymer and *R* the gas constant. Wendling and Suter have recently proposed a model to describe the melting point depression in random copolymers in a frustrated thermodynamic equilibrium.[32] In the limit of complete comonomer exclusion [that is, where ϵ/RT is relatively large (ϵ is the excess defect free energy)], their model reduces to

$$\frac{1}{T_m^{0\prime}} - \frac{1}{T_m^0} = \frac{-R}{\Delta H_f^0}(\ln X_S - 1/\xi) \tag{7}$$

where ξ is the average sequence length of both monomers and is equal to $[2X_S(1 - X_S)]^{-1}$ for random copolymers.[33] Equation 7 is the same as that arrived at by Baur a number of years ago.[34]

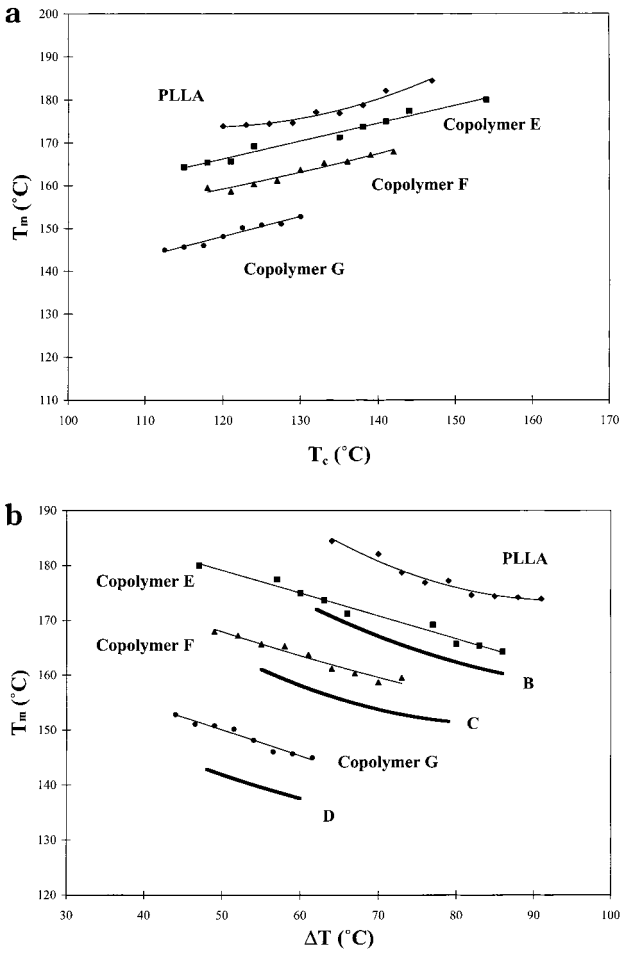

Figure 5. (a) Experimental T_m's vs T_c. PLLA (◆), copolymers E (■), F (▲), and G (●). **(**b**)** T_m as a function of ΔT. PLLA (◆), copolymers E (■), F (▲), and G (●). Data for *meso*-lactide copolymers from ref 13.

For the case of uniform inclusion of *R* stereoisomers into *S* crystals, Sanchez and Eby arrived at[35]

$$T_m^{0'} = T_m^0\left(1 - \frac{\epsilon}{\Delta H_f^0} X_R\right) \qquad (8)$$

where X_R is the mole fraction of *R* stereochemical species.

Values for $T_m^{0'}$ predicted from these expressions are summarized in Table 2. The values for the uniform inclusion model were calculated assuming $\epsilon = 2.45$ kJ/mol comonomer units, a value proposed for D-lactide defects in *S* stereoisomer crystals.[35] In addition, the heat of fusion for crystals in which *R* defects are included is expected to be reduced from that of crystals containing no such defects. However, for copolymers with relatively low defect mole fraction, like those under consideration here, only a small decrease in ΔH_f^0 would be expected, and ΔH_f^0 was considered to be a constant for purposes of the calculations that resulted in the values in Table 2.

The calculations of the melting point depression are straightforward for the *meso*-lactide copolymers, with their lone, randomly placed counits. However, defining the mole fraction of the defective units in the D-lactide copolymers in a consistent fashion presents a more difficult problem. Taking X_R strictly as the mole fraction of *R* units for the D-lactide copolymers overcounts the number of defects. On the other hand, defining the mole fraction of defects in a manner consistent with the *meso*-lactide copolymers underestimates the importance of defect size in the D-lactide copolymers. Thus, there are two entries listed under each model in Table 2 for the D-lactide copolymers: the first is a "lower bound" calculated from the total *R* content, and the second is an "upper bound" based on the number of defects/100 monomer units, ignoring defect size.

The calculated equilibrium melting points for the *meso*-lactide copolymers from the Flory exclusion and uniform inclusion models are significantly larger than those determined experimentally, particularly for copolymers C and D. However, the predicted values in the exclusion limit of the model of Wendling and Suter[32] fit the data very well. For the D-lactide copolymers, the calculated $T_m^{0'}$ (lower and upper bounds) from the Flory exclusion and uniform inclusion models are significantly larger than the experimental values. The range of values calculated from the Wendling−Suter model in the exclusion limit are again relatively close to the experimental values. Taken together with the significant reduction in lamellar thickness observed with increasing D-lactide or *meso*-lactide concentration, these results point to significant rejection of *meso*- and D-lactide defects from the *S* crystals.

However, there is NMR and other evidence that at least some *R* (or *R*−*R*) counits can be included in *S* crystals under certain crystallization conditions.[36,37] In addition, NMR evidence also supports some inclusion of stereochemical defects in crystals of polymers like polypropylene.[38] How then can we reconcile the equilibrium melting points of the poly(lactide) copolymers? Crystallization was conducted relatively slowly in our experiments, perhaps kinetically trapping less *R*−*R* (or *R*) species in crystalline regions. Fitting eq 8 to the *meso*-lactide copolymer data leads to a value for ϵ on the order of $1.4\Delta H_f^0$. Relatively large excess defect free energies have been reported for other copolymers previously (obtained by fitting eq 8 to experimental data),[39,40] but a value of $\epsilon/\Delta H_f^0 \sim 1.4$ seems to be particularly large, considering that the *R* counits have the same chemical makeup as the *S* species. For example, $\epsilon/\Delta H_f^0$ was estimated to be about 0.2 for isotactic polypropylene containing stereochemical defects.[22] Calculation of the potential energy of *R* and *R*−*R* stereochemical defects in *S* crystals is currently underway.

Spherulite Growth Rates. As noted earlier, spherulitic growth rates were determined for all materials over a range of T_c's. These data are summarized in Figure 6, along with similar data from ref 13 for the *meso*-lactide copolymers. Since $T_m^{0'}$ decreases with increasing comonomer content (and T_g is constant), the window of crystallization for the copolymers is compressed with increasing X_R. In addition, there is about an order of magnitude reduction in the maxima growth rate at the highest comonomer content: ∼4.8 μm/min for PLLA to 0.54 μm/min for copolymer G. The importance of defect arrangement is reflected in the growth rates: at equivalent *R* stereoisomer content, growth rates for the D-lactide copolymers are significantly higher than for the corresponding *meso*-lactide copolymers (copolymers E vs B, F vs C, and G vs D). Growth rates are generally somewhat depressed for the copolymers with the bulkier D-lactide defects (copolymers B vs F and C vs G).

The Lauritzen−Hoffman−Miller kinetic model was used to analyze the growth rate data for poly(L-lactide).

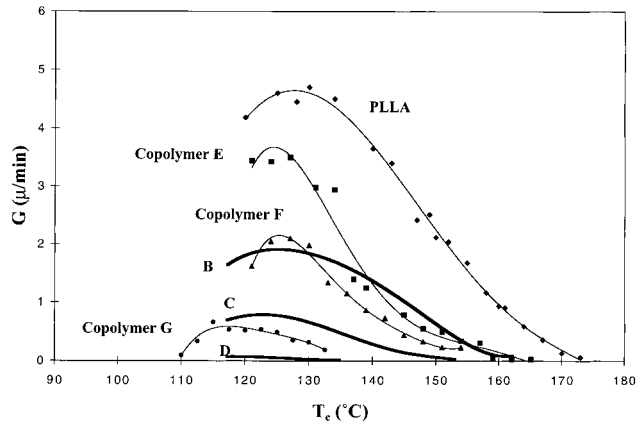

Figure 6. Spherulite growth rates for D-lactide copolymers. PLLA (◆), copolymers E (●), F (▲), and G (●). Data for *meso*-lactide copolymers from ref 13.

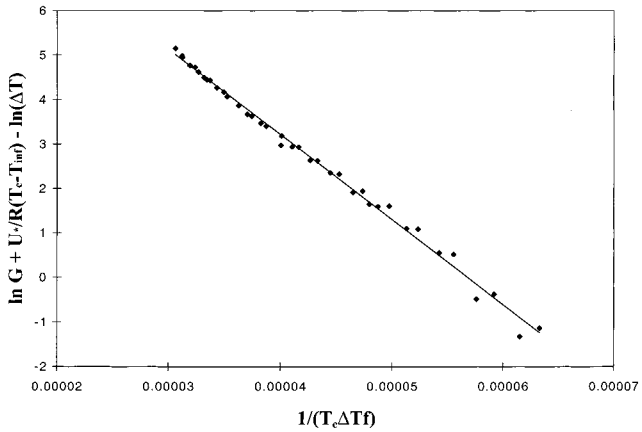

Figure 7. LH plot for poly(L-lactide). Data pooled from Figure 6 and ref 13.

The data for the copolymers were not analyzed in this way since, as noted earlier, the usual form of LHM model does not completely account for the influence of comonomer on lamellar thickness. The relationship between the growth rate and factors related to transport and secondary nucleation can be written as[28]

$$G = G_0(\Delta T) \exp(-U^*/R(T_c - T_\infty)) \exp(-K_g/T_c(\Delta T)f) \quad (9)$$

where U^* is the activation energy for transport, R the gas constant, T_∞ the temperature below which viscous flow stops (taken here as $T_g - 30$ K), K_g the nucleation constant, and f a correction factor which accounts for the variation in the perfect crystal heat of fusion with temperature. K_g is defined as $n_i b_0 \sigma \sigma_e T_m^0 / k \Delta H_f^0$, where n_i is 4 for crystallization regimes I and III and 2 for regime II, b_0 the layer thickness, σ the lateral surface free energy, and k the Boltzmann constant.

The LH plot for PLLA for data pooled from Figure 6 and from ref 13 is presented in Figure 7. In the analysis U^* was taken as the "universal" value of 1.5 kcal/mol, $b_0 = 0.517$ nm,[29] and crystalline and amorphous densities of 1.29 and 1.25 g/cm^3, respectively.[36] Note that there is no regime break observed in Figure 7. The fitted values of K_g from the slope and ln G_0 from the intercept of the LH plot are 1.92×10^5 K^2 and 10.9, respectively. For growth in regime II,[13] $\sigma\sigma_e = 682$ erg^2/cm^4. Taking $\sigma = 12$ erg/cm^2 [29] yields 57 erg/cm^2. This value is in excellent agreement with the independent Gibbs–Thomson estimate of σ_e (63 erg/cm^2) as well as with the earlier estimate of Hoffman et al.[30]

Conclusions

Cross-polarized optical microscopy, SAXS, and DSC were used to investigate the influence of random D-lactide defects on crystallization and the solid-state structure of three poly(L-lactide-*co*-D-lactide) polymers. As expected, these copolymers exhibit a significant decrease in bulk crystallinity with modest D-lactide incorporation. At equivalent *R* stereoisomer content, φ_c (D-lactide copolymers) > φ_c (*meso*-lactide copolymers), illustrating the importance of defect arrangement (i.e., paired vs isolated) on the development of crystallinity. In addition, at equivalent comonomer content, the larger D-lactide defects lead in general to a greater reduction in φ_c compared to *meso*-lactide defects at the same ΔT. Likewise, there is a significant reduction in spherulite growth rate with increasing D-lactide content, and the importance of defect arrangement was again demonstrated by comparison to our earlier research on L-lactide/*meso*-lactide copolymers.

At a given ΔT, the lamellar thickness derived from SAXS experiments was found to be significantly reduced with increasing defect concentration. This behavior is consistent with the limited, defect-free crystallizable sequence lengths available in copolymers with higher *R* stereoisomer contents.

SAXS and optical microscopy experiments lead to the following model of the solid-state structure of the D-lactide copolymers. The superstructure is spherulitic (~5−30 μm diameter in our case), and the spherulites contain significant pockets of noncrystalline material between stacks of lamellae. The fraction of the amorphous component residing between lamellar stacks was found to decrease with decreasing ΔT for PLLA and the D-lactide copolymers. For PLLA, the fraction of interfibrillar amorphous material ranges from ~40 to 60%.

Equilibrium (and experimental) melting points were found to decrease significantly with increasing comonomer content. Predicted equilibrium melting points in the exclusion limit of the model of Wendling and Suter[32] fit the data for D-lactide and *meso*-lactide copolymers well. Taken together with the significant reduction in lamellar thickness with increasing D-lactide (or *meso*-lactide) concentration, these results point to significant rejection of *meso*- and D-lactide defects from *S* stereoisomer crystals. However, evidence presented by other authors[36,37] supports some D-lactide (or *meso*-lactide) incorporation in *S* crystals under certain crystallization conditions. Some speculation about the origin of these different conclusions is presented.

Acknowledgment. We express our appreciation to the donors of the ACS Petroleum Research Fund for their support of this research. This research was also supported in part by the Division of Materials Sciences, U.S. Department of Energy, under Contract DE-AC05-00OR22725 with the Oak Ridge National Laboratory, managed by UT-Battelle, LLC. Finally, we thank James Garrett for helpful discussions.

References and Notes

(1) Hauser, G.; Schmidtke, J.; Strobl, G. *Macromolecules* **1998**, *31*, 6250.
(2) Crist, B.; Howard, P. R. *Macromolecules* **1999**, *32*, 3057.
(3) Androsch, R.; Blackwell, J.; Chavalun, S. N.; Wunderlich, B. *Macromolecules* **1999**, *32*, 3735.

(4) Isasi, J. R.; Haigh, J. A.; Graham, J. T.; Mandelkern, L.; Alamo, R. G. *Polymer* **2000**, *41*, 8813.
(5) Hill, M. J.; Barham, P. J. *Polymer* **2000**, *41*, 1621.
(6) Saragusa, J. R.; Prud'homme, R. E.; Wisniewski, M.; Le Borgne, A.; Spassky, N. *Macromolecules* **1998**, *31*, 3895.
(7) Chisholm, M. H.; Iyer, S. S.; McCollum, D. G.; Pagel, M.; Werner-Zwanziger, U. *Macromolecules* **1999**, *32*, 963.
(8) Li, S. M.; McCarthy, S. *Macromolecules* **1999**, *32*, 4454.
(9) Palade, L. I.; Lehermeier, H. J.; Dorgan, J. R. *Macromolecules* **2001**, *34*, 1384.
(10) Langer, R.; Vacanti, J. P. *Science* **1993**, *260*, 920.
(11) Zhang, X.; Goosen, M. F. A.; Wyss, U. P.; Pichora, D. *J. Macromol. Sci., Rev. Macromol. Chem. Phys.* **1993**, *C33*, 81.
(12) Vert, M.; Schwarch, G.; Coudane, J. *J. Macromol. Sci., Pure Appl. Chem.* **1995**, *A32*, 787.
(13) Huang, J.; Lisowski, M. S.; Runt, J. P.; Hall, E. S.; Kean, R. T.; Buehler, N.; Lin J. S. *Macromolecules* **1998**, *31*, 2593.
(14) Runt, J.; Huang, J.; Lisowski, M. S.; Hall, E.; Kean, R.; Lin, J. S. In *Polymers from Renewable Materials, Biopolyesters and Biocatalysis;* ACS Symposium Series 764; Scholtz, C., Gross, R. A., Eds.; American Chemical Society: Washington, DC, 2000; Chapter 15.
(15) Thakur, K. A. M.; Kean, R. T.; Hall, E. S.; Kolstad, J. J.; Lindgren, T. A.; Doscotch, M. A.; Siepmann, J. I.; Munson, E. J. *Macromolecules* **1997**, *30*, 2422.
(16) Kricheldorff, H. R.; Dunsing, R. *Makromol. Chem.* **1986**, *187*, 1611.
(17) Painter, P. C.; Coleman, M. M. *Fundamentals of Polymer Science*; Technomic Publishing: Lancaster, PA, 1994.
(18) Hsiao, B. S.; Verma, R. K. *J. Synchrotron Rad.* **1998**, *5*, 23.
(19) Vonk, C. G. *J. Appl. Crystallogr.* **1973**, *6*, 81.
(20) Vonk, C. G.; Kortleve, G. *Kolloid Z. Z. Polym.* **1967**, *220*, 19.
(21) Strobl, G. R.; Schneider, M. *J. Polym. Sci., Polym. Phys. Ed.* **1980**, *18*, 1343.
(22) Cheng, S. Z. D.; Janimak, J. J.; Zhang, A.; Hsieh, E. T. *Polymer* **1991**, *32*, 648.
(23) Talibuddin, S.; Wu, L.; Runt, L.; Lin J. S. *Macromolecules* **1996**, *29*, 7527.
(24) Kanchanasopa, M.; Runt, J. Unpublished data.
(25) Hoffman, J. D.; Davis, G. T.; Lauritzen, J. I., Jr. In *Treatise on Solid State Chemistry*; Hanny, N. B., Ed.; Plenum Press: New York, 1976; Vol. 3, Chapter 7.
(26) Alamo, R. G.; Viers, B. D.; Mandelkern, L. *Macromolecules* **1995**, *28*, 3205.
(27) Marand, H.; Xu, J.; Srinivas, S. *Macromolecules* **1998**, *31*, 8219.
(28) Hoffman, J. H.; Miller, R. L. *Polymer* **1997**, *38*, 3151.
(29) Vasanthakumar, R.; Pennings, A. J. *Polymer* **1983**, *24*, 175.
(30) Hoffman, J. D.; Miller, R. L.; Marand, H.; Roitman, D. B. *Macromolecules* **1992**, *25*, 2221.
(31) Flory, P. J. *Trans. Faraday Soc.* **1955**, *51*, 848.
(32) Wendling, J.; Suter, U. W. *Macromolecules* **1998**, *31*, 251.
(33) Wunderlich, B. *Macromolecular Physics*; Academic Press: New York, 1980; Vol. 3.
(34) Baur, H. *Makromol. Chem.* **1966**, *98*, 297.
(35) Sanchez, I. C.; Eby, R. K. *Macromolecules* **1975**, *8*, 638.
(36) Fischer, E. W.; Sterzel, H. J.; Wegner, G. *Kolloid Z. Z. Polym.* **1973**, *251*, 980.
(37) Zell, M. T.; Padden, B. E.; Paterick, A. J.; Hillmyer, M. A.; Kean, R. T.; Thakur, K. A. M.; Munson, E. J. *J. Am. Chem. Soc.* **1998**, *120*, 12072.
(38) VanderHart, D. L.; Alamo, R. G.; Nyden, M. R.; Kim, M. H.; Mandelkern, L. *Macromolecules* **2000**, *33*, 6078.
(39) Kim, M. H.; Phillips, P. J.; Lin, J. S. *J. Polym. Sci., Polym. Phys.* **2000**, *38*, 154.
(40) Dikshit, A. K.; Nandi, A. K. *J. Polym. Sci., Polym. Phys.* **2000**, *38*, 297.

MA001125R